Modeling of the Compression Process for Refrigerants R134a and R1234yf of a Variable Speed Reciprocating Compressor

J.M. Barroso-Maldonado, J.M. Belman-Flores* and S. Ledesma

Engineering Division, Campus Irapuato-Salamanca, University of Guanajuato, Salamanca, Gto., CP.36885, México

Abstract: This paper presents a robust computational model to predict the behavior of a variable speed reciprocating compressor, incorporating infinitesimal displacements to calculate state by state according to the piston movement. The philosophy of the model is to consider eight sub internal processes: heat transfer on the suction and discharge internal lines, pressure drop across the suction and discharge valves, expansion, suction, compression and discharge. The input variables are: pressure and temperature on the suction (before starting the compression process), discharge pressure (after the compression process completed) and rotation speed, with this the model is able to compute the output parameters like: mass flow rate, power consumption and discharge temperature. With the development of the model, the behaviors of R1234yf and R134a are analyzed. Then the model is validated with experimental data using these both refrigerants, concluding that the model predict with an error of ±10% for the mass flow rate and power consumption, and with an error of ±1 K for the discharge temperature. In the validation, differences in energy behavior for the two refrigerants are discussed; the compressor with R1234yf as working fluid increases its power consumption and delivers greater mass flow rate with low temperature compared when the working fluid on the compressor is R134a.

Keywords: Vapour compression, refrigeration, energy, thermodynamic analysis.

1. INTRODUCTION

Currently, there are several technologies to produce artificial cold; one of most widespread is based on the vapour compression system. In this type of refrigeration, the refrigerant is a substance that absorbs heat at low pressure and low temperature. This heat is transferred to a sink medium at high pressure and high temperature. The basic components of a vapour compression system are: condenser, expansion valve, evaporator and compressor. In these systems, the analysis and research of the compressor and the working fluid (refrigerant) are very important, because the compressor consumes energy in the refrigeration systems; furthermore the refrigerant causes certain harmful effects on the environment.

The refrigerants, Chlorofluorocarbons (CFCs) and hydrochlorofluorocarbons (HCFCs) introduced in the thirties and fifties, respectively, were defined as main contributors to ozone depletion, years after, they were displaced by hydrofluorocarbons (HFCs) that have zero ozone depletion, with the R134a belonging to this group. However, since the R134a provides a high Global Warming Potential (GWP), currently R1234yf which belongs to the group of hydrofluoro olefin (HFO), is one of the best candidates to replace it due to its environmental benefits such as its GWP of 4 and 11 days life in the atmosphere compared to a GWP of 1430 and 14 years of life in the atmosphere of R134a. In this context, Minor and Spatz [1] presented a detail study of the characteristics of both refrigerants. Thermodynamic studies of the behavior of R1234yf are presented in references [2-4]. A summary of some thermophysical properties for both refrigerants are presented in Table **1**.

Table 1: Summary of some Thermophysical Properties

Property	R1234yf	R134a
Boiling point (K)	244.15	247.15
Critical point	368.15	375.15
Evaporating pressure at 298.15 K (MPa)	0.677	0.665
Condensing pressure at 353.15 K (MPa)	2.44	2.63
Liquid density at 298.15 K (kg m^{-3})	1094	1207
Vapor density at 298.15 K (kg m^{-3})	37.6	32.4

As shown in Table **1**, the main refrigerant thermodynamic properties, quantitatively are very similar for both. The R1234yf has a higher vapor density and lower liquid density than R134a.

In the literature, there are studies that analyze the overall behavior of R1234yf. For instance in Zilio *et al*. [5], they experimentally analyzed an automotive air conditioning; their results show that for the system with R1234yf the overall COP is lower when compared to the COP produced with R134a. Similarly, Navarro et al. [6] presented a study where a vapor compression system is experimentally analyzed by checking the energy differences between R134a and R1234yf. They

*Address correspondence to this author at the Engineering Division, Campus Irapuato-Salamanca, CP. 36885. México; Tel: 01464 6479940;
Fax: +52 (464) 6479940 Ext. 2311; E-mail: jfbelman@ugto.mx

E-ISSN: 2409-5826/15

obtained reductions of 9% for cooling capacity and 19% for COP when R1234yf was the working fluid. On another study, Navarro *et al*. [7] showed the analysis of a vapor compression system affected by an internal heat exchanger; the purpose of their work was to assess its effect on the energy performance of the system when R1234yf was used, and compare it to the performance when using R134a without the internal heat exchanger. From the experimental results, reductions in cooling capacity and COP are between 6% and 13% when R134a is replaced by R1234yf, although the presence of the internal heat exchanger helps to lessen these reductions between 2% and 6%. Ledesma and Belman *et al*. [8] presented an artificial neural network to model a vapor compression system using R1234yf, the model was oriented to compute the coefficient of performance. In the literature, different types of modeling for compressors are presented, from those that solve the equations of conservation of mass, momentum and energy [9-11] to those models that are aided by empirical correlations [12-15]. However, empirical correlations are for certain compressor and under specific conditions, so sometimes is necessary to expand the analysis and involve geometric features and operating conditions. Navarro *et al*. [16] developed a model for a reciprocating compressor dividing the process in internal sub-processes and considering a polytropic process. In order to test the model, it is applied on another research for different compressors; through experimental validation it is shown that the topology of the model is adequate only when certain empirical parameters are known [17]. In the research of Duprez *et al.* [18], a model for reciprocating compressors is presented. The model is able to predict both the mass flow rate and the power consumption; the model was tested with five compressors with capacity of 10 kW under different refrigerants. The authors divide the compression process in five internal subprocesses: heat transfer in suction and discharge line, pressure drop in the suction and discharge valve, and an isentropic compression process. Therefore, the geometry and some operating conditions play an important role in the equations, for example: the diameter of the suction line, the rotation speed, the dead volume, the stroke and the cylinder wall temperature; each being fixed values within the simulation. The same idea of dividing the compression process in internal subprocesses is also used by Winandy *et al*. [19]; the novelty of the investigation is the consideration of the power loss by friction in compression process. This loss is mathematically proposed as a function of rotation speed, and then, within the first law of thermodynamics the heat transfer across cylinder walls was incorporated. Yang *et al*. [20] analyzed the friction losses involving a kinematic model for the reciprocating motion, and incorporated a thermal analysis considering the heat transfer to the cylinder walls by Newton's law of cooling. The heat transfer coefficient has been studied in the literature and empirical correlations for calculation are exposed [21-23].

The robustness of compressor modeling allows knowing the effect of certain parameters and especially to get the actual operation of the compressor close to the system of equations obtained from physical

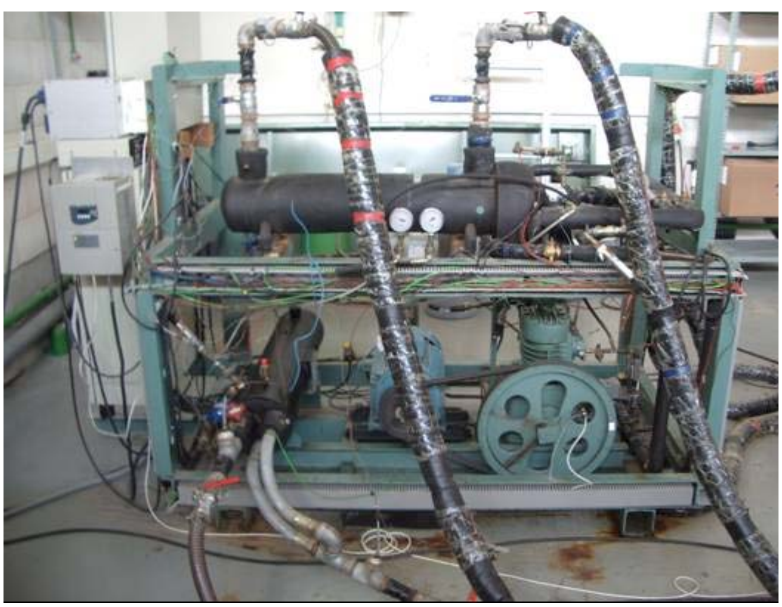

Figure 1: Test facility of the vapor compression system.

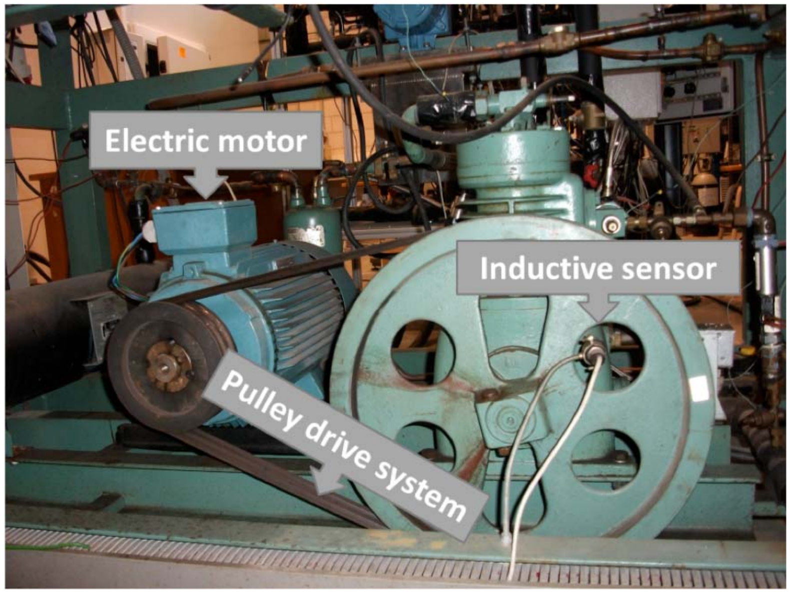

Figure 2: Reciprocating compressor open type.

phenomena. In this context, this paper presents a model of reciprocating compressor, in this case, the input variables are: the rotation speed, the pressure and the temperature of the refrigerant in the suction line and the discharge pressure. The model predicts: the volumetric efficiency, the refrigerant mass flow rate, the power consumption, and the discharge temperature of the refrigerant. The compression process is divided into eight sub-processes: heat transfer and pressure drop both in the suction line as in the discharge, expansion, suction, compression, discharge. Certain thermodynamic states are subsequently generated by infinitesimal displacements of the piston. As novelty, for each state a thermodynamic analysis is carried out until the compression process is completed. The proposed model is used to compare the energy performance for both refrigerants: R134a and R1234yf.

2. EXPERIMENTAL FACILITY

The experimental facility of the vapor compression system is depicted in Figure **1**.

The system on this Figure consists of one vapor compression circuit (in a single-stage compression) and two secondary fluids circuits. The main circuit has: an open type variable speed compressor, a shell-and-tube evaporator, a shell-and-tube condenser, and a thermostatic expansion valve. The test facility is fully instrumented to measure variables such as pressure, temperature, mass flow rate, rotation speed and power consumption. The circuit is adapted to work with different refrigerants; this includes R407C, R134a and R1234yf. The volumetric flow and the inlet temperature of the secondary fluid and the rotational speed are the controllable parameters in the experimental tests. The compressor mounted on this circuit is an open type Bitzer V model (see Figure **2**). These compressors have a shell which is independent of the electrical engine so that the connection to the motor is made through a mechanical transmission by pulleys. In Table **2**, some technical parameters of this component are presented.

Table 2: Geometrical Features of the Compressor

Number of cylinders	2
Piston diameter [m]	0.085
Stroke [m]	0.060
Rotation speed range [rpm]	400-600
Diameter-length of the internal suction line [m]	0.029-0.06
Diameter-length of the internal discharge line [m]	0.029-0.06
Displaced volume [m^3/h] @ 560 [rpm]	23.1

Various types of sensors are strategically located, depending on the parameter to be measured, in close proximity to the compressor obtaining records for the variables of interest such as: temperature, pressure, mass flow rate, rotation speed and power consumption. Table **3** presents a summary of the type of sensors used and the uncertainty associated with each measurement. The signals generated by these sensors are directed to a SCXI 1000 data acquisition system from National Instrument.

Table 3: Measured Parameters and Uncertainty

Parameter	Instrument	Uncertainty
Temperature	Thermocouple K-type	±0.3K
Pressure	Pressure transducers	±0.1%
Power	Digital wattmeter	±0.5%
Mass flow rate	Coriolis flow-meter	±0.22%
Rotation speed	Inductive sensor	±1%

3. PHYSICAL MODEL

The compression process is depicted in the *P-h* diagram of Figure **3**. The refrigerant goes into the compressor at point 1 with suction conditions; the final thermodynamic state indicated by the number 6 represents the discharge conditions. According to this, the model assumes that the progress of the refrigerant through the compressor can be divided into the following steps:

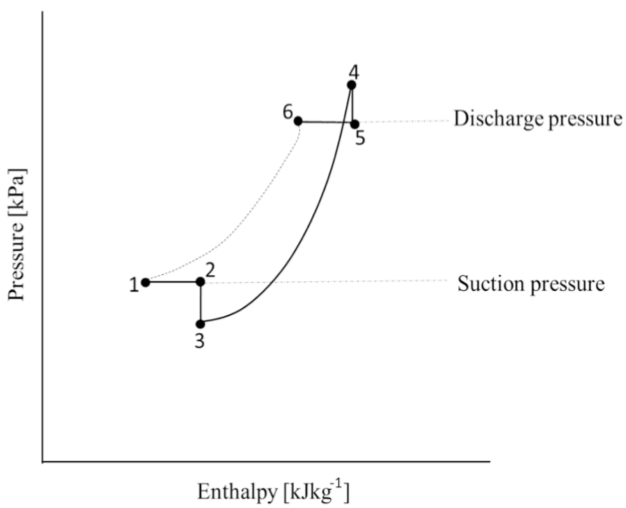

Figure 3: Diagram *p-h* of the compression process.

- Internal flow heat transfer at suction line (1-2)
- Isenthalpic pressure drop at suction valve (2-3)
- Compression process (3-4)
  - Expansion
  - Suction
  - Compression
  - Discharge
- Isenthalpic pressure drop at discharge valve (4-5)
- Internal flow heat transfer at discharge line (5-6)

The main contribution of this paper is how the compression process (3-4) is recalculated using the thermodynamic states produced by the infinitesimal movements of the piston. The considerations that have been made are listed below:

- The process of expansion, suction, compression and discharge, are divided into internal threads, which are considered in this work as quasi-static processes.
- The model considers only steady-state behavior in the operation of the compressor.

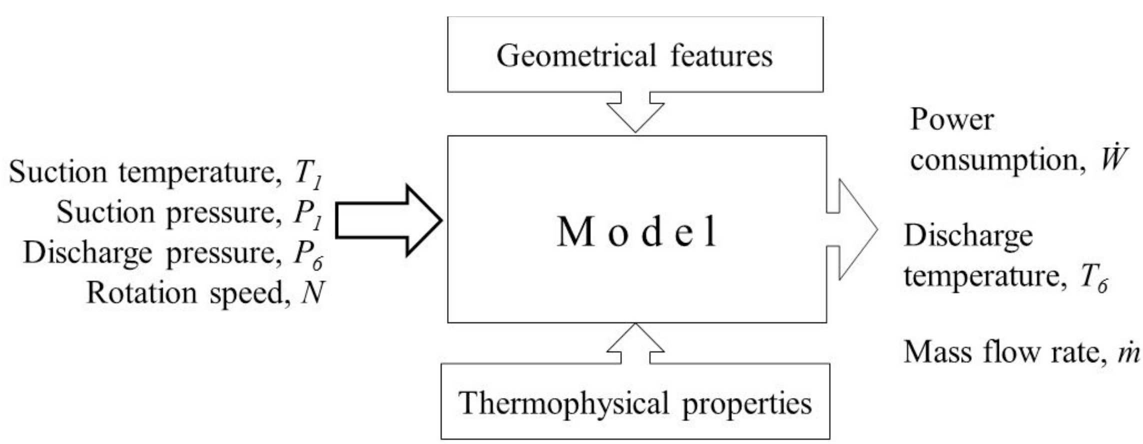

Figure 4: Modeling a compression process.

- Oil leaks to the compression chamber are ignored.
- The condensing refrigerant in proximity to the suction valve is neglected.

Figure **4** represents the model structure indicating the input variables and estimated parameters. Also, the model requires knowing the following geometric characteristics of the compressor: the diameter of the suction and discharge line, the diameter of the cylinder, the stroke and the dead space.

3.1. Heat Transfer: Internal Suction and Discharge Line

To calculate the temperatures at points 2 and 6 (affected by the heat transfer in the suction and discharge line, respectively) Eq. 1 is used [24]:

$$\frac{T_w - T_{2,6}}{T_w - T_{1,5}} = \exp\left[-\frac{\pi D L}{\dot{m} C_p} \bar{h} \right]. \tag{1}$$

The heat transfer convective coefficient is estimated by Petukhov correlation [25], defined as:

$$\bar{h} = \left(\frac{k}{D} \right) \frac{\left(f/8 \right) \mathrm{Re}\,\mathrm{Pr}}{1.07 + 12.7 \left(f/8 \right)^{1/2} \left(\mathrm{Pr}^{2/3} - 1 \right)}, \tag{2}$$

where the friction factor may be obtained from f=[0.79ln(Re)-1.64]$^{-2}$.

3.2 Isenthalpic Pressure Drop at the Suction and Discharge Valve

When the fluid flows through the valve there is always a spring force trying to close the passage, this phenomenon causes a pressure loss throughout the suction and discharge, to quantify the pressure drop various models have been proposed in the literature, ranges that stand out are 5 kPa to 40 kPa and 70 kPa to 200 kPa, for suction and discharge respectively. To compute this parameter we use the equation proposed by Winandy *et al*. [19] as shown in Eq. 3 for suction, ΔP_s, and Eq. 4 for discharge, ΔP_d:

$$\Delta P_s = \frac{\left(\dfrac{4\dot{m}}{0.0196 \pi V_{swept}} \right)^2}{a \rho_s}, \tag{3}$$

$$\Delta P_d = b + c \left(\frac{\dot{m}}{d} \right)^2, \tag{4}$$

where, according to the author, the constants have the following values: a=2000, b=100, c=300, d=0.02, units are kPa.

3.3. Heat Transfer Across Cylinder Walls

The temperature of the refrigerant contained within the cylinder varies along of the cycle because the thermodynamic state is given by the instantaneous position of the piston; thus the temperature difference is not the same throughout the cycle and therefore the heat transfer is not either. The Newton's law of cooling is the adequate physical concept for this phenomenon:

$$\dot{q}(t) = h(t)\; A(t) \left[T(t) - T_w \right]. \tag{5}$$

The convective coefficient is obtained from the Nusselt number as shown in Eq. 6.

$$h(t) = \frac{k(t)}{D_p} a \; \mathrm{Re}(t)^b \; \mathrm{Pr}(t)^c. \tag{6}$$

In Table **4**, the Reynolds number and the coeff-icients are exposed according to the process undergone by the refrigerant [22].

Table 4: Reynolds Number According to the Process Undergone by the Refrigerant

Process	Reynolds Number	Coefficients
Expansion	$\mathrm{Re}(t) = \frac{\rho(t)\, D\, V_p}{\mu(t)}$	*a=0.12, b=0.8, c=0.6*
Suction	$\mathrm{Re}(t) = \frac{\rho(t) D \left(V_p + V_p^{-0.4} V_c(t)^{1.4} \right)}{\mu(t)}; V_c(t) = \frac{\lvert \dot{m}(t) \rvert}{\rho(t)\, A_c}$	*a=0.8, b=0.9, c=0.6*
Compression	$\mathrm{Re}(t) = \frac{\rho(t)\, D\, V_p}{\mu(t)}$	*a=0.8, b=0.8, c=0.6*
Discharge	$\mathrm{Re}(t) = \frac{\rho(t) D \left(V_p + V_p^{0.8} V_c(t)^{0.2} \right)}{\mu(t)}; V_c(t) = \frac{\lvert \dot{m}(t) \rvert}{\rho(t)\, A_c}$	*a=0.08, b=0.9, c=0.6*

3.4. Expansion

Certain amount of refrigerant is contained in the dead space with high pressure and temperature, it exerts a force on the frontal face of the piston causing it to move and thereby starting expansion; to analyze all sub-processes that integrate the expansion, the first law of thermodynamics is applied as illustrated

$$\left.\frac{dE}{dt}\right|_{v.c.} = \dot{Q}_{v.c.} - \dot{W}_{v.c.} + \sum_{input} \dot{m}\left(i + \frac{V^2}{2} + gz\right) - \sum_{output} \dot{m}\left(i + \frac{V^2}{2} + gz\right). \quad (7)$$

The effects of the kinetic and the potential term are ignored. As the valves are closed, the equation describing the process from state t to state $t+\Delta t$ is:

$$m\frac{e(t+\Delta t) - e(t)}{\Delta t} = \dot{Q}_{t \to t+\Delta t} - \frac{1}{\Delta t}\int_t^{t+\Delta t} PdV. \quad (8)$$

In the Eq.8 m is the mass that is expanding, Δt is the time took for the piston to travel the infinitesimal displacement Δx and e is the internal energy which is recalculated for states $t+\Delta t$ achieving fully define each state. The expansion stops when suction pressure is bigger than the internal pressure plus the pressure drop across the suction valve, immediately after the suction begins.

3.5. Suction

The process called suction is when the refrigerant comes into the cylinder while the piston goes to the lower dead point; the suction volume, $V_{Suction}$, is defined as the volume occupied to do this movement. Because the total geometric volume of the cylinder, V_{Swept}, and the volume occupied by the expansion, $V_{Expansion}$, are known, the volumetric efficiency is defined as:

$$\eta_{vol} = \frac{V_{Swept} - V_{Expansion}}{V_{Swept}} = \frac{V_{Suction}}{V_{Swept}}. \quad (9)$$

This relationship is used to obtain the mass flow rate as follows:

$$\dot{m} = \rho_{suction} V_{Swept} \frac{N}{60} \eta_{vol}. \quad (10)$$

The suction is considered as a sequence of quasistatic sub-processes, thus, the same philosophy employed for the expansion is used in the suction, compression and discharge. Therefore, in the following sections only the equations were specified according to the process conditions. In this case for suction, the first law of thermodynamics reduces to:

$$m\frac{e(t+\Delta t) - e(t)}{\Delta t} = \dot{Q}_{t \to t+\Delta t} - \frac{1}{\Delta t}\int_t^{t+\Delta t} PdV + \dot{m}i, \quad (11)$$

where $\dot{m}i$ represents the enthalpy times that the mass flow that crosses the boundaries of the control volume representing the cylinder, the sign is positive and is negative when it comes in or when it comes out of the control volume, respectively. The pressure and temperature of the refrigerant in the cylinder are computed when the piston is located at the lower dead point; this thermodynamic state is the initial for the compression process described below.

3.6. Compression

The compression process starts when the piston makes the infinitesimal displacement Δx in the opposite direction reducing the volume of the mass contained; with the valves closed the pressure increase is achieved. Eq. 8 helps to determine all thermodynamic states while the piston is compressing the refrigerant. The pressure and temperature is increased in each quasistatic sub-state until a desired pressure is achieved; this can overcome the pressure drop in the discharge valve plus the discharge pressure and thus the refrigerant leaves the cylinder. The total work required for the compression process can be calculated as the work done during the compression process minus the work gained on the expansion, expressed as follows [26]:

$$W = \int_{Comp} VdP - \int_{Exp} VdP. \quad (12)$$

3.7. Discharge

The method used in the suction also applies to the discharge; however, the appropriated form to the first law contains a negative sign in the last term (the product of the enthalpy and mass flow rate). The pressure and temperature of the refrigerant in the cylinder are computed when the piston is located at the upper dead point; this thermodynamic state is for the refrigerant stored on the clearance volume which is ready to begin with the expansion and re-start the whole compression cycle.

Having the complete model, the system of equations is programmed in the EES software (Engineering Equation Solver) to solve the output parameters that Figure **4** suggests. The flowchart of Figure **5** represents the solution algorithm for the reciprocating compressor.

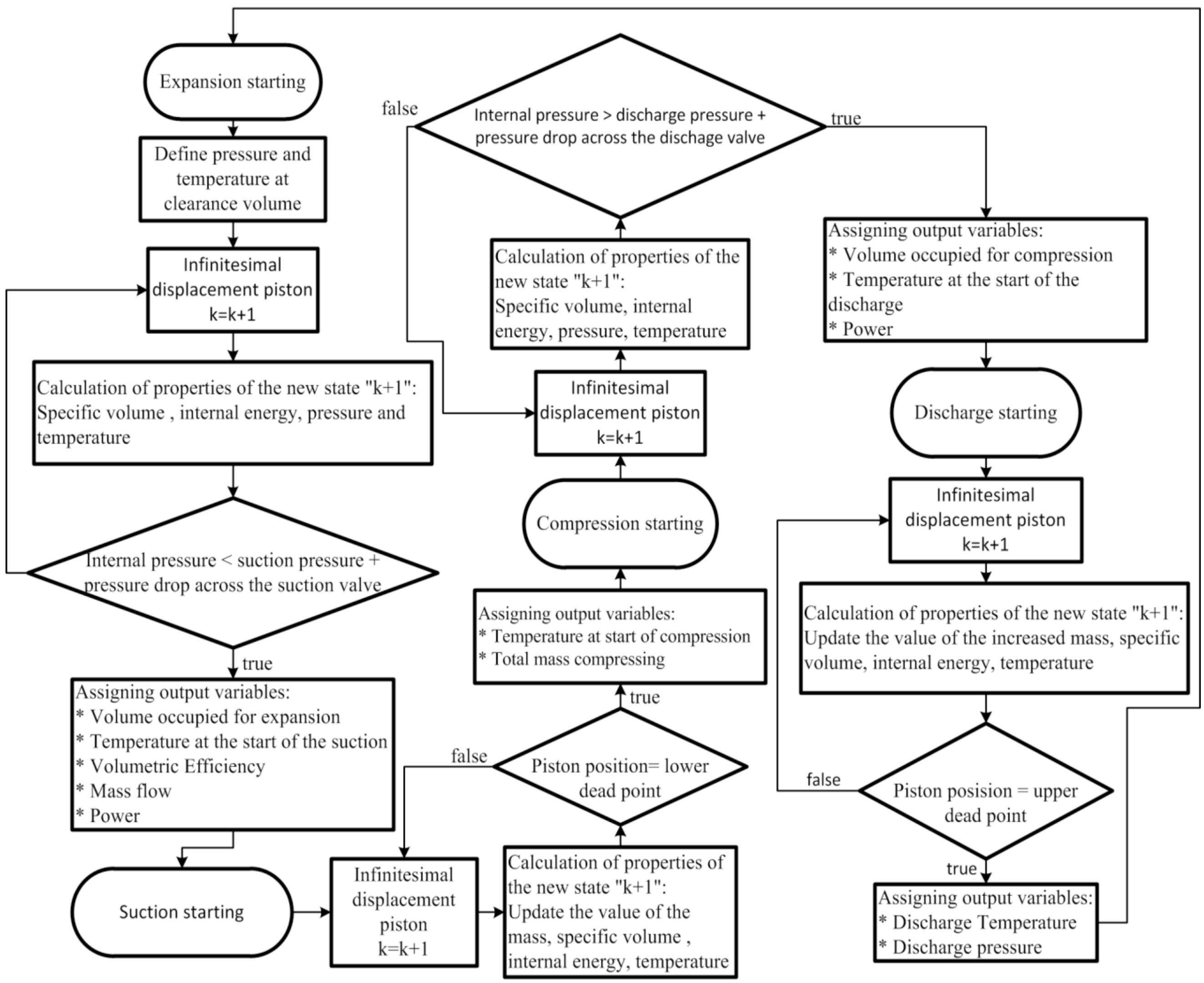

Figure 5: Proposed algorithm.

4. RESULTS

To validate the developed model, a comparison between experimental data and model outputs is carried out. The geometric characteristics of the compressor are reviewed in Table **2**. It is important to mention that the instrumentation is not included in the cylinder walls, so does not have relevant information on the wall temperature; however the literature suggests assigning a constant value for this parameter [18-20]. For this work the value for the temperature that the oil returns to the compressor is 328K.

When the model is solved, the results are compared with experimental tests. Suction pressure, suction temperature, discharge pressure along with the geometrical features are used as input variables. The first output parameter is the mass flow rate showed in Figure **6**. According to this Figure, the model is well validated for the mass flow rate, within ±10% deviation respect to the experimental data. Given that most of the data for both refrigerants are contained within this range, it is assumed that the model is adequate for predicting the mass flow rate.

The calculated discharge temperature for both refrigerants has a good approximation as it can been seen in Figure **7**, the lines representing ±1 K error are over plotted in the same Figure being the computed data inside of this range. More than 95% of computed data are within this range.

Figure **8** shows the prediction for compressor power consumption. The predicted parameter agrees quite well with the experimental value because the error is about ±10%, and approximately 95% of the data are within this range.

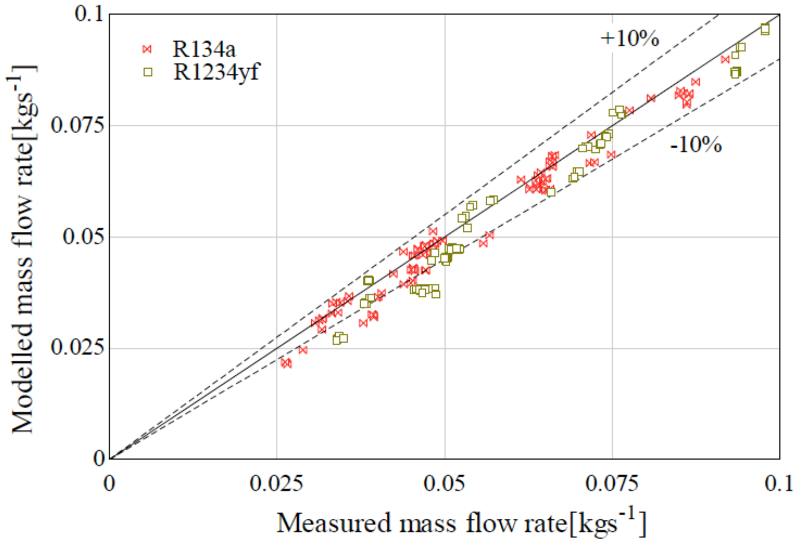

Figure 6: Prediction of mass flow rate.

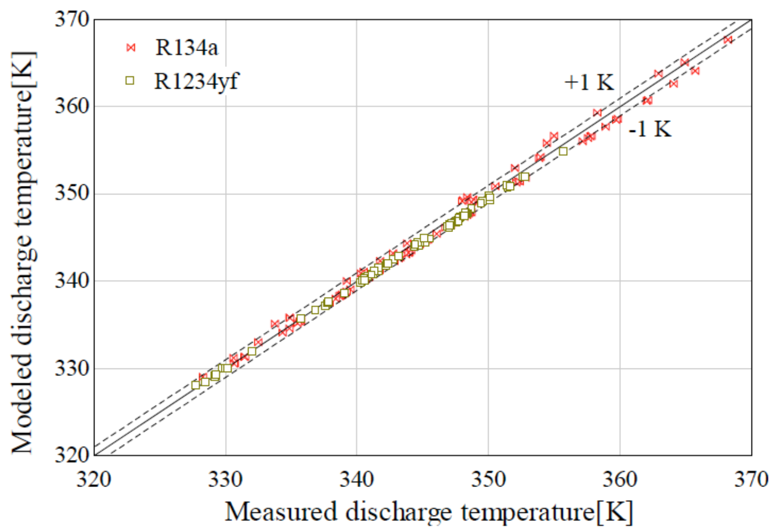

Figure 7: Prediction of discharge temperature.

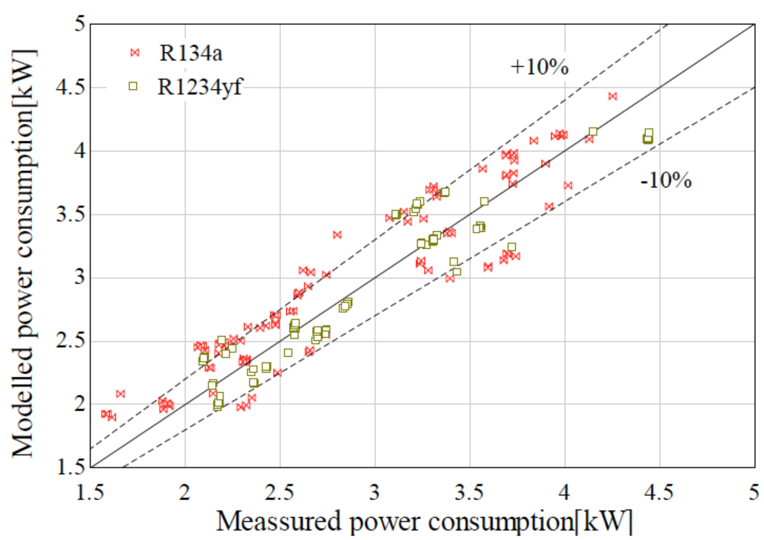

Figure 8: Prediction of power consumption.

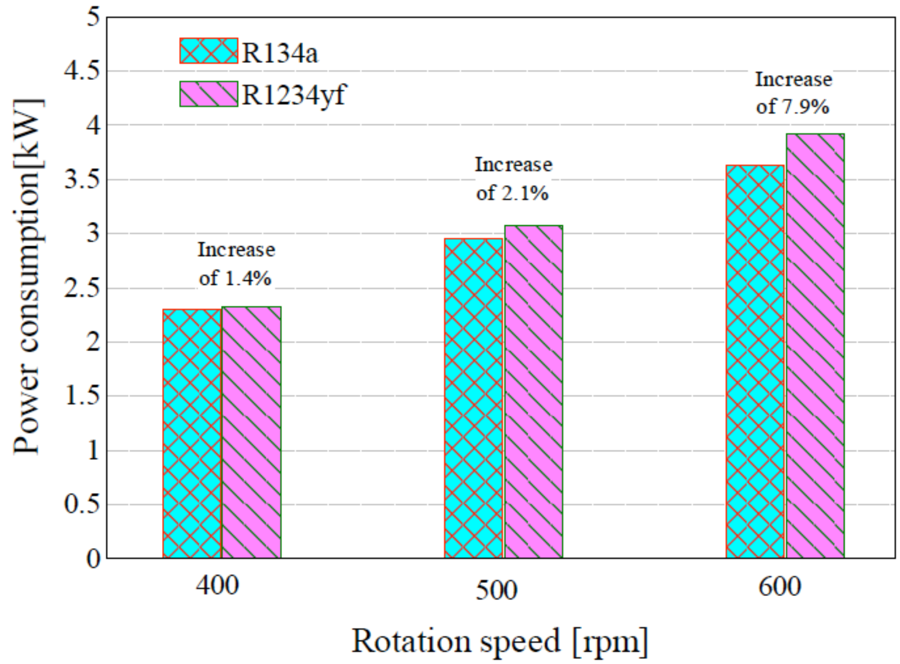

Figure 9: Estimating the power consumption.

4.1. Energetic Simulation

In order to establish the differences in power consumption for both refrigerants, the model is carried out to an energy simulation. Under the same operating conditions by varying the rotation speed, the power consumption is calculated in this simulation.

For the simulation the variables chosen are: P_1=250 kPa, T_1=280 K, P_6=1200 kPa, respectively correspond to the suction pressure, suction temperature and discharge pressure. For these conditions three different rotation speeds are proposed: 400, 500 and 600 rpm. Given the same cooling capacity, in Figure **9** clearly shows that the compressor working with R1234yf represents a lower energy efficiency compared to R134a. In other words, the power consumption with R1234yf is greater than R134a. For low rotation speed the power consumption increases 1.4% for R1234yf, for the intermediate rotation speed this increment is 2.1% and for the high rotation speed this increment is 7.9%. Thus, at low rotation speeds, very similar energy consumption is achieved, in this particular case and also due to the electromechanical characteristics of the compressor; the best performance of the experimental test facility would be achieved. On the other hand, when the compressor is operated at high speeds, the energy performance is not appropriated, particularly because the R1234yf does increase power consumption. Therefore, it is not recommended to operate the compressor at high rotation speeds with R1234yf. So energy improvements currently are studied with this refrigerant.

5. CONCLUSIONS

A physical model to predict the behavior of a reciprocating compressor is presented. The analysis consists of dividing the whole process into eight sub internal processes: heat transfer and pressure drop across the suction and discharge, expansion, suction, compression and discharge. The procedure algorithm is aimed to calculate each of the thermodynamic states while the piston performs infinitesimal displacements. The model is able to compute parameters of first importance such as mass flow rate, power consumption and discharge temperature. The model is examined through an experimental validation for two refrigerants: R1234yf and R134a. Results show ±10% of relative error for the mass flow rate and power consumption, and an error of ±1 K for the discharge temperature. Despite similarities between the thermophysical properties between these refrigerants, certain differences in the operating conditions are presented. The model is used to simulate the power consumption of this compressor for both refrigerants. When the compressor works at low rotation speed the differences of power consumption are 1.4%, and when it operates at high rotation speed the differences of power consumption are 7.9%. For R1234yf the power consumption is greater than R134a, however, if the compressor is working at low rotation speeds, the power consumption no presents significant differences for both refrigerants.

ACKNOWLEDGMENTS

To the University of Guanajuato through the "Integral Institutional Strengthening Program" (PIFI 2013).

NOMENCLATURE

A	Area, $[m^2]$
C_p	Specific heat, $[J\ kg^{-1}\ K^{-1}]$
D	Diameter for suction and discharge internal lines, [m]
e	Internal energy, $[J\ kg^{-1}]$
L	Length of the suction and discharge internal lines, [m]
h	Convective heat transfer coefficient, $[Wm^{-2}K^{-1}]$
i	Enthalpy, $[J\ kg^{-1}]$
k	Thermal conductivity, $[W\ m^{-1}\ K^{-1}]$
T_w	Wall temperature, [K]
t	Time, [s]
Vswept	Total geometric volume of the cylinder, $[m^3]$
Vp	Piston velocity, $[m\ s^{-1}]$
Pr	Prandtl number
Re	Reynolds number
Δ	Difference
μ	Dynamic viscosity, [Pa s]
ρ	Density, $[kg\ m^{-3}]$

REFERENCES

[1] Minor B, Spatz M. HFO-1234yf Low GWP Refrigerant Update. International Journal and Air Conditioning Conference 2008; pp 1-8.

[2] Akasaka R, Tanaka K, Higashi Y. Thermodynamic property modeling for 2,3,3,3 tetrafluoropropene (HFO-1234yf). International Journal of Refrigeration 2010; 33: pp 52-60. http://dx.doi.org/10.1016/j.ijrefrig.2009.09.004

[3] Tanaka K, Higashi Y. Thermodynamic properties of HFO-1234yf (2,3,3,3-tetrafluoropropane). International Journal of Refrigeration 2010; 33: pp 474-479. http://dx.doi.org/10.1016/j.ijrefrig.2009.10.003

[4] Lai N, Vrabec J, Raabe G, Fischer J, Wendland M. Description of HFO-1234yf with BACKONE equation of state. Fluid Phase Equilibria 2011; 305: pp 2014-2020. http://dx.doi.org/10.1016/j.fluid.2011.04.005

[5] Zilio C, Steven B, Schichet G, Cavallini A. The refrigerant R1234yf in air conditioning systems. Energy 2011; 36: pp 6110-6120. http://dx.doi.org/10.1016/j.energy.2011.08.002

[6] Navarro E, Mendoza J, Mota A, Barragán A, Belman JM. Experimental analysis of R1234yf as a drop-in replacement or R134a in a vapor compression system. International Journal of Refrigeration 2013; 36: pp 870-880. http://dx.doi.org/10.1016/j.ijrefrig.2012.12.014

[7] Navarro E, Molés F, Barragán C. Experimental analysis of the internal heat exchanger influence on a vapour compression system performance working with R1234yf as a drop-in replacement for R134a. Applied Thermal Engineering 2013; 59: pp 153-161. http://dx.doi.org/10.1016/j.applthermaleng.2013.05.028

[8] Ledesma S, Belman-Flores JM. Application of artificial neural networks for generation of energetic maps of a variable speed compression system working with R1234yf. Applied Thermal Engineering 2014; 69: pp 105-112. http://dx.doi.org/10.1016/j.applthermaleng.2014.04.050

[9] Damle R, Rigola J, Pérez C, Castro J, Oliva A. Object-oriented simulation of reciprocating compressors: Numerical verification and experimental comparison. International Journal of Refrigeration 2011; 34: pp 1989-1998. http://dx.doi.org/10.1016/j.ijrefrig.2011.02.006

[10] Rigola J, Pérez CD, Oliva A. Parametric studies on hermetic reciprocating compressors. International Journal of Refrigeration 2005; 28: pp 253-266. http://dx.doi.org/10.1016/j.ijrefrig.2004.06.013

[11] Peskin A. The effects of different property models in a computational fluid dynamics simulation of a reciprocating compressor. International Journal of Thermophysics 1999; 20: pp 175-186. http://dx.doi.org/10.1023/A:1021442616990

[12] Matos F, Prata A, Deschamps C. A numerical methodology for the analysis of valve dynamics. Proceedings of the International Compressor Engineering Conference. Purdue 2000; 391-396.

[13] Libera, Faraon, Solari. A complete analysis of dynamic behavior of hermetic compressor cavity to improve the muffler design. Proceedings of the International Compressor Engineering Conference. Purdue 2000; pp 665-669.

[14] Ma Y, Min O. On study of pressure pulsation using a modified Helmholtz method. Proceedings of the International Compressor Engineering Conference. Purdue 2000; pp 657-664.

[15] Gonzalves J, Hermes C, Melo C, Knaben F. A simplified steady state model for prediction the energy consumption of household refrigerators and freezers. International Refrigeration and Air Conditioning Conference at Purdue 2008; pp 1-9.

[16] Navarro E, Granryd E, Urchueguía JF, Corberán J. A phenomenological model for analyzing reciprocating compressors. International Journal of Refrigeration 2007; 30: pp 1254-1265. http://dx.doi.org/10.1016/j.ijrefrig.2007.02.006

[17] Navarro E, Granryd E, Urchueguía JF, Corberán J. Performance analysis of a series of hermetic reciprocating working with R290 (propane) and R407C. International Journal of Refrigeration 2007; 30: pp 1254-1265. http://dx.doi.org/10.1016/j.ijrefrig.2007.02.006

[18] Duprez M, Dumont E, Frere M. Modelling of reciprocating and scroll compressors. International Journal of Refrigeration 2007; 30: pp 873-886. http://dx.doi.org/10.1016/j.ijrefrig.2006.11.014

[19] Wynandi E, Saavedra O, Lebrun J. Simplified modelling of an open type reciprocating compressor. International Journal of Thermal Science 2002; 41: pp 183-192. http://dx.doi.org/10.1016/S1290-0729(01)01296-0

[20] Yang B, Bradshaw C, Groll E. Modeling of a semi-hermetic CO2 reciprocating compressor including lubrication sub-models for piston rings and bearings. International Journal of Refrigeration 2012; 30: pp 1-13.

[21] Fagotti, Prata. A New Correlation for Instantaneous Heat Transfer Between Gas and Cylinder in Reciprocating Compressors. International Compressor Engineering Conference, Purdue 1998; pp 871-876.

[22] Disconzi F, Deschamps C, Pereira E. Development of an In-Cylinder Heat Transfer Correlation for Reciprocating Compressors. International Compressor Engineering Conference, Purdue 2012; pp 1-10.

[23] Adair R, Qvale E, Pearson J. Instantaneous heat transfer to the cylinder wall in reciprocating compressors. International Compressor Engineering Conference, Purdue 1972; pp 521-526.

[24] Incropera FP, Dewitt DP, Bergman TL, Lavine AS. Introduction to Heat Transfer. 5th Edition. John Wiley and Sons 2007.

[25] Petukhov BS, Popov VN. Theoretical calculation of heat exchange and frictional resistance in turbulent flow in tubes of an incompressible fluid with variable physical properties (Heat exchange and frictional resistance in turbulent flow of liquids with variable physical properties through tubes). High Temperature 1963; 1: pp 69-83.

[26] Hanne E. Tetchiness Thermodynamic. Addison-Wesley Publishing Company. Bonn. 2nd Edition 1993.

Received on 04-10-2014 Accepted on 23-10-2014 Published on 15-01-2015

DOI: http://dx.doi.org/10.15377/2409-5826.2015.02.01.5